Volume 8 – Issue 85
Issued on: 20 November 2026
International Journal of Research and Studies Publishing
المجلة الدولية لنشر البحوث والدراسات
ISSN: 2709-7064

Assessing Urban Thermal Stress Effects on Date Palm Agroecosystems in Al-Ahsa Oasis Using Remote Sensing Indicators (2017–2024)

Nawaf Nader[a], Alyaa A. Zidan[b,c], Rawan A. Nughaymish[d], Basim Al Sahabi[e]

[a] Department of Geography, PhD Candidate in Environmental Studies, Qassim University, Buraidah, Saudi Arabia

[b] National Institute of Oceanography and Fisheries (NIOF), Cairo, Egypt

[c] State Key Laboratory of Marine Geology, Tongji University, Shanghai 200092, China

[d] Department of Biology, Princess Nourah bint Abdulrahman University, Riyadh, Saudi Arabia

[e] Department of Environmental Engineering, Umm Al-Qura University, Makkah, Saudi Arabia

Corresponding author Email: a: nawaf.a.nader@gmail.com

Abstract:

This study investigates the spatiotemporal dynamics of urban thermal stress on date palm agroecosystems in Al-Ahsa Oasis, Eastern Province, Saudi Arabia, over the period 2017–2024. Using multi-temporal Landsat 8/9 and Sentinel-2 satellite imagery processed in Google Earth Engine (GEE), Land Surface Temperature (LST), the Normalized Difference Vegetation Index (NDVI), and the Normalized Difference Moisture Index (NDMI) were analyzed across 89.69 km² of palm farm vegetation. Results indicate a mean LST increase of +1.81°C in palm-farm pixels within the Near Urban zone (0–500 m from built-up areas) over the study period, with spatially heterogeneous warming concentrated along the eastern urban fringe. Pearson correlation analysis (n = 727 palm-farm pixels) revealed a substantially stronger negative relationship between LST and NDMI ($r = -0.599$, $p < 0.001$, $R^2 = 0.359$) than between LST and NDVI ($r = -0.316$, $p < 0.001$, $R^2 = 0.100$), indicating that canopy moisture content responds more directly to thermal exposure than vegetation greenness in this irrigated system. Spatial analysis demonstrated that moisture stress hotspots were concentrated within fragmented urban–agricultural interface zones, where elevated temperatures coincided with declining vegetation condition. These findings provide a quantitative basis for spatially targeted conservation interventions and urban planning strategies aligned with Saudi Vision 2030 and the UNESCO Outstanding Universal Value of Al-Ahsa Oasis.

Keywords: Urban Heat Island; Date Palm; Al-Ahsa Oasis; Land Surface Temperature; NDVI; NDMI; Google Earth Engine; Remote Sensing; Saudi Arabia; Thermal Stress

1. Introduction

Urbanization is transforming Earth's surface, with 68% of the global population projected to reside in urban areas by 2050 (United Nations, 2018). Impervious materials replace permeable surfaces, generating the Urban Heat Island (UHI) phenomenon. Surface UHI intensities in arid environments can exceed 10–12°C during summer, with the sharpest contrasts at agricultural-urban interfaces (Hassaballa & Salih, 2023). Lazzarini et al. (2013) confirmed that arid-region cities exhibit the highest UHI intensities globally due to differences in radiative properties between vegetated and built surfaces. Date palm (*Phoenix dactylifera* L.) agroecosystems are particularly susceptible to UHI-induced thermal stress. Historically, these systems produced localized "Oasis Cool Island" effects, decreasing local temperatures by 5–8°C through canopy shading and evapotranspiration (Boudjellal et al., 2025; Boudjellal & Bourbia, 2018). Progressive urban encroachment systematically dismantles these cooling mechanisms (Salih et al., 2025).

Recent research has advanced the understanding of date palm heat-stress responses. Yaish and Halo (2026) identified key heat shock protein (HSP) genes that confer thermotolerance by maintaining cellular protein homeostasis. de Souza et al. (2025) revealed that sustained moderate heat stress (37°C) inhibits isoprene synthase activity while reprogramming carbon flux through the MEP pathway. At the physiological level, Paoletti et al. (2021) documented that chronic stress reduces the maximum quantum yield of photosystem II (Fv/Fm), accelerates chlorophyll degradation, and diminishes photosynthetic pigment content. Kruse et al. (2019) demonstrated that date palm shifts its optimum photosynthesis temperature from 20–33°C (winter) to 28–45°C (summer) while maintaining tight coupling between stomatal conductance and photosynthetic rates. The emergence of Date Fruit Unripening Syndrome (DFUS) provides production-level evidence: Iqbal et al. (2025) documented that DFUS affects 20–30% of date production, preventing normal Rutab-to-Tamar transition, strongly associated with daytime temperatures reaching 48°C during critical fruit development stages.

Remote sensing enables reproducible assessment of vegetation health. The Normalized Difference Vegetation Index (NDVI) and Normalized Difference Moisture Index (NDMI) are widely validated for stress detection. Gao (1996) established NDMI using shortwave infrared reflectance for water-content sensitivity, and recent studies have confirmed its utility for date palm assessment (Salih et al., 2025). For Land Surface Temperature (LST) retrieval, Sekertekin and Bonafoni (2020) validated split-window algorithms for Landsat 8/9 (RMSE ~1.5–2.0 K), while Avdan and Jovanovska (2016) established operational LST mapping protocols. Sishodia et al. (2020) demonstrated that NDVI-LST-

NDMI frameworks detect crop stress before visible symptoms emerge. Google Earth Engine (GEE) has transformed large-scale geospatial analysis by providing cloud-based access to Landsat and Sentinel-2 archives (Gorelick et al., 2017).

Despite substantial research, no study has directly correlated urban-derived LST with date palm NDVI and NDMI using a spatial proximity stratification framework in Al-Ahsa Oasis. Existing research characterized urban expansion without linking to vegetation health (Almadini & Hassaballa, 2019), mapped UHI without distance stratification (Hassaballa & Salih, 2023), or assessed spectral indices without quantifying urban proximity effects (Salih et al., 2025). This study addresses this gap by: (1) mapping LST from Landsat 8/9 thermal imagery; (2) computing date palm health indices (NDVI and NDMI) from Sentinel-2 and Landsat imagery; (3) quantifying the statistical relationships between thermal exposure and vegetation stress indicators using correlation analyses; and (4) delivering evidence-based recommendations for oasis conservation aligned with Saudi Vision 2030 objectives.

2. Study Area

The Al-Ahsa Oasis is located in Saudi Arabia's Eastern Province (25°23′–25°30′N, 49°33′–49°43′E), approximately 60 km inland from the Arabian Gulf (Figure 1). The study boundary spans approximately 49.41°E to 49.78°E and 25.28°N to 25.56°N, covering the major urban-agricultural interface zones within the oasis. The hyper-arid climate features extremely hot summers (mean maximum 42–46°C, extremes exceeding 48°C in July–August), mild winters (minimums averaging 8–12°C), and mean annual precipitation below 100 mm. Relative humidity ranges from 5% (summer afternoons) to 96% (winter nights).

Al-Ahsa is one of the largest and oldest continuously cultivated date palm systems globally, with agricultural activity spanning more than 5,000 years (UNESCO, 2018). Designated a UNESCO World Heritage Site in 2018, the oasis encompasses approximately 8,500 cultivated hectares supporting 2.5–3.0 million date palms across more than 40 cultivars, with 'Khalas' comprising approximately 50% of total yield. The twin metropolitan centers of Al-Hofuf and Al-Mubarraz constitute the urban core, with a combined population of approximately 1.1 million in 2022, representing a 45% increase from 2010 (Hassaballa & Salih, 2023). Built-up areas increased from 17.15% to 45.8% of total land use between 1990 and 2020 (a 170% proportional increase), with approximately 1,700 hectares of date palm plantations converted to urban uses over this period. Salih et al. (2025) confirmed, using Spectral Mixture Analysis, that urbanization—not climate or soil factors—was the primary driver of palm cover loss, with the most intense conversion occurring within a 2 km radius of urban boundaries.

Volume 8 – Issue 85
Issued on: 20 November 2026
International Journal of Research and Studies Publishing
المجلة الدولية لنشر البحوث والدراسات
ISSN: 2709-7064

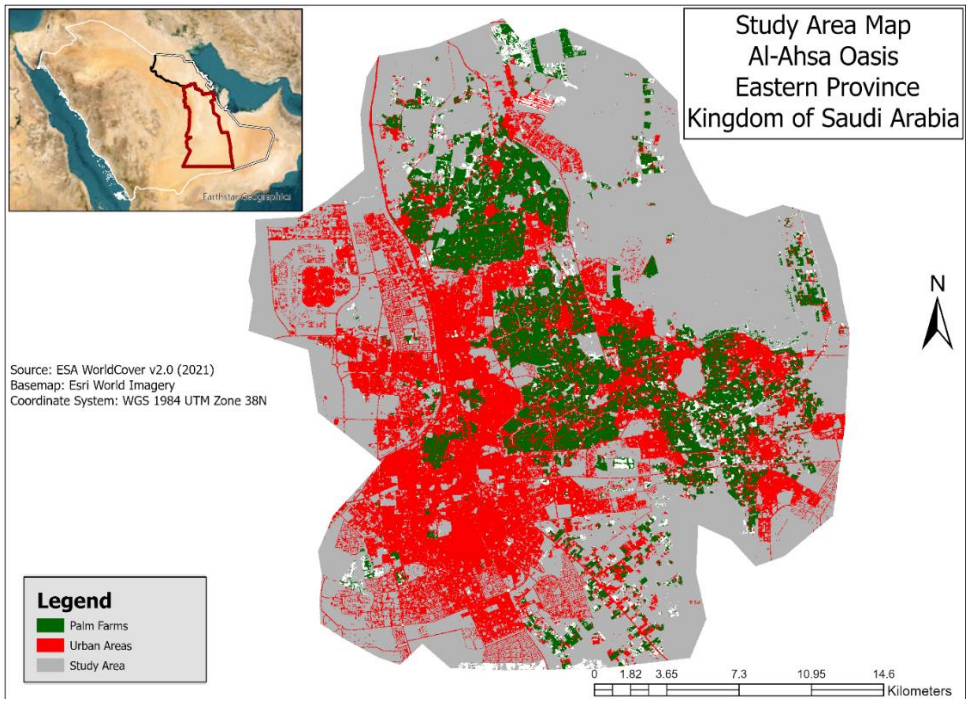

Figure 1. Study Area Map showing the spatial distribution of land cover classes within Al-Ahsa Oasis, Eastern Province, Kingdom of Saudi Arabia. The study area encompasses approximately 89.69 km² of palm-farm vegetation (green; ESA WorldCover class 10, see Section 3.1) interspersed with extensive urban and built-up areas (red; class 50), derived from ESA WorldCover v2.0 (2021). The oasis is situated within the Hofuf–Mubarraz metropolitan corridor.

3. Materials and Methods

3.1. Remote Sensing and GIS-Based Spatial Analysis

This study employed remote sensing and Geographic Information System (GIS) techniques to investigate the spatial relationship between urban thermal intensity and date palm stress indicators in Al-Ahsa Oasis. Multi-source satellite datasets from Landsat 8/9 OLI/TIRS and Sentinel-2 MSI were processed using Google Earth Engine (GEE) and ArcGIS Pro. Landsat Collection 2 Level-2 and Sentinel-2 SR Harmonized products were used, which are atmospherically corrected by the data providers. Sentinel-2 scenes with less than 15% cloudy pixels were additionally masked for clouds and cirrus using the QA60 band, Landsat scenes were filtered to less than 10% scene-level cloud cover, and summer (1 May–30 September) pixel-wise mean composites were clipped to the study boundary.

Date palm-cultivated areas were delineated from the ESA WorldCover v2.0 (2021) 10 m land-cover product, which has no dedicated date palm class. Pixels classified as Tree cover (class 10) within the oasis boundary were extracted and treated as palm-farm vegetation, since date palm is the main tree

crop of Al-Ahsa Oasis (Almadini & Hassaballa, 2019; Salih et al., 2025); no additional spectral threshold was applied. The resulting mask covers 89.69 km². Built-up areas were extracted from class 50 (Built-up). Because the mask represents 2021 conditions and was applied to both 2017 and 2024 imagery, changes in palm extent between these dates are not captured.

Urban expansion zones were delineated from ESA WorldCover v2.0 (2021) built-up land-cover classifications. An initial design of five proximity buffer classes (0–100, 100–250, 250–500, 500–1,000, and >1,000 m from urban boundaries) was applied to evaluate thermal influence gradients on surrounding palm agroecosystems. However, the deeply intermingled spatial configuration of palm farms and urban fabric in Al-Ahsa Oasis resulted in very few palm pixels beyond 500 m from built-up areas (878 pixels, 0.8% of palm pixels, at 500–1,500 m; 3 pixels beyond 1,500 m). For analytical purposes, buffer classes were therefore consolidated into two primary zones: Near Urban (0–500 m; 110,516 palm pixels, 722 in the random sample) and Medium Urban (500–1,500 m; 878 palm pixels, 5 in the sample). Results for the Near Urban zone are statistically robust; those for the Medium Urban zone are presented as exploratory evidence only, given the small sample size.

3.2. Land Surface Temperature (LST) Retrieval

LST was derived from Landsat 8/9 thermal infrared bands using established remote sensing procedures (Avdan & Jovanovska, 2016; Sekertekin & Bonafoni, 2020). Landsat Collection 2 Level-2 surface temperature products (ST_B10) were converted from Kelvin to degrees Celsius using the scaling factors provided by the United States Geological Survey (USGS). Surface thermal maps were generated to identify thermal hotspots and assess spatial patterns of heat exposure across palm agroecosystems. Summer LST composites (1 May–30 September) were computed as the mean of Landsat 8 (2017) and Landsat 9 (2024) scenes with less than 10% cloud cover. Zonal LST statistics (Table 1) were computed over all palm-farm pixels at 30 m resolution. For the correlation analyses, 5,000 random points (seed = 42) were generated over the study area at 30 m, and the 727 points falling on palm-farm pixels were retained, with LST, NDVI, and NDMI values for summer 2024 extracted at these points.

3.3. Vegetation Health and Moisture Stress Indices

Date palm health conditions were assessed using spectral indices derived from Sentinel-2 and Landsat imagery. The Normalized Difference Vegetation Index (NDVI) was used to estimate vegetation vigour and photosynthetic activity:

$$NDVI = (NIR - Red) / (NIR + Red)$$

(Sentinel-2 bands B8 and B4)

Canopy moisture conditions were evaluated using the Normalized Difference Moisture Index (NDMI):

$$NDMI = (NIR - SWIR) / (NIR + SWIR)$$

(Sentinel-2 bands B8A and B11)

Higher NDVI values indicate healthier vegetation, while lower NDMI values indicate moisture deficiency and increased stress (Gao, 1996; Karnieli et al., 2010). NDMI was classified into four categories: Severe Water Stress (< -0.07), Mild Water Stress (-0.07 to < 0.12), Moderate Moisture (0.12 to 0.25), and High Moisture (> 0.25). These thresholds were adapted from Gao (1996) to the observed data range of this study.

3.4. Statistical Analysis

Statistical analyses were conducted using Microsoft Excel. Descriptive statistics (mean, standard deviation, minimum, and maximum) were calculated for LST, NDVI, and NDMI. Pearson product–moment correlation coefficients were used to quantify relationships among the environmental variables. Statistical significance was assessed at the $\alpha = 0.05$ level.

3.5. Software and Analytical Platforms

The analytical workflow was implemented using: Google Earth Engine (GEE), ArcGIS Pro, and Microsoft Excel. Google Earth Engine was used for satellite image processing and extraction of LST, NDVI, and NDMI. ArcGIS Pro was used for spatial analysis, buffer-zone generation, and cartographic visualization. Microsoft Excel was used for statistical calculations including descriptive statistics, Pearson correlation.

4. Results

4.1. Land Cover Configuration and Buffer Zone Distribution

Palm farm vegetation covers an estimated 89.69 km² within the defined study boundary, constituting the primary agricultural and heritage land cover class. ESA WorldCover v2.0 (2021) confirms that palm farms and built-up areas are spatially intermingled throughout the oasis, with no large contiguous blocks of palm farm vegetation separated from urban land use by distances exceeding 1,500 m. This spatial configuration resulted in 99.3% of the 727 randomly sampled palm-farm pixels falling within the Near Urban proximity zone (0–500 m from built-up surfaces), confirming that Al-Ahsa Oasis cannot be treated as a conventional rural agricultural landscape separated from urban influence.

4.2. Spatiotemporal Variation in Land Surface Temperature

The spatial distribution of LST during summer 2017 and 2024 is shown in Figure 2. LST values across the full study area (including all land cover types) ranged from 36.52°C to 58.14°C in 2017 and from 36.91°C to 61.51°C in 2024, reflecting general thermal intensification over the study period. Within palm-farm areas specifically, descriptive statistics by proximity zone are provided in Table 1.

In the Near Urban zone, mean LST across all palm-farm pixels (n = 110,516) increased from 45.16°C in 2017 to 46.97°C in 2024, representing a rise of +1.81°C. The Medium Urban zone recorded consistently higher mean LST values (52.31°C in 2017; 50.98°C in 2024). These values—higher than the Near Urban zone—are interpreted with caution and are discussed in Section 5.6. This counterintuitive pattern—where the zone farther from urban boundaries records higher LST—is likely driven by the limited extent of palm pixels in this zone (0.8% of palm pixels, n = 878) and mixed-pixel exposure to surrounding desert surfaces, rather than a genuine distance-based thermal gradient. The Far Urban zone (n = 3 pixels) is excluded from inferential analysis due to insufficient sample size; its elevated LST values most likely reflect the thermal influence of surrounding bare soil and desert surfaces rather than urban proximity per se.

Table 1. Descriptive Statistics of LST (°C) for All Palm-Farm Pixels by Urban Proximity Zone (2017 & 2024)

Zone	Year	n	Mean (°C)	Max (°C)	Min (°C)	SD (°C)
Near Urban	2017	110,516	45.16	55.73	37.26	2.95
Near Urban	2024	110,516	46.97	57.60	38.87	2.93
Medium Urban	2017	878	52.31	55.26	48.58	1.08
Medium Urban	2024	878	50.98	56.69	47.38	1.94
Far Urban*	2017	3	54.53	55.12	53.68	0.62
Far Urban*	2024	3	56.56	57.14	55.39	0.82

*Far Urban zone (n = 3) is excluded from all inferential analyses due to insufficient sample size. Elevated LST values in this zone likely reflect bare soil and desert surface heating rather than urban proximity. Note: Table 1 reports all palm-farm pixels (ESA WorldCover v2.0 class 10, 30 m grid) in each proximity zone (full population, not a sample); no other land-cover types are included.

Table 2 reports statistics for a random sample of these palm-farm pixels (n = 727) for summer 2024. SD = Standard Deviation. Source: USGS Landsat 8/9 Level-2, Collection 2, processed via Google Earth Engine.

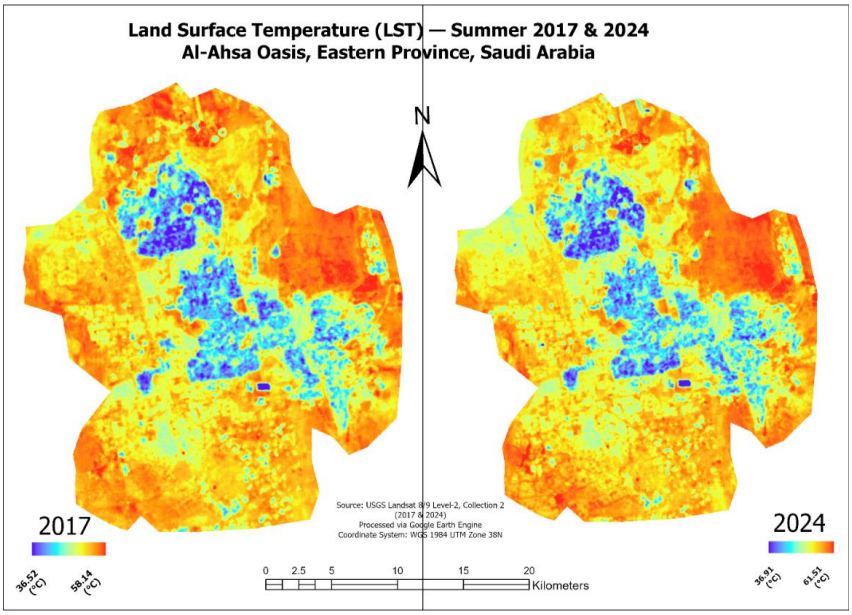

Figure 2. Spatial distribution of Land Surface Temperature (LST) in Al-Ahsa Oasis during summer 2017 (a) and 2024 (b). LST values across the full study area ranged from 36.52°C to 58.14°C in 2017 and from 36.91°C to 61.51°C in 2024. Note that these full-area ranges include non-vegetated surfaces (bare soil, built-up areas); LST statistics for palm-farm pixels only are presented in Tables 1 and 2. Lower LST values (blue tones) are concentrated over dense palm farm clusters; higher values (red-orange) dominate peripheral bare soil and built-up areas.

4.3. Vegetation Condition in Urban Proximity Zones

Table 2 presents descriptive statistics for LST, NDVI, and NDMI derived from 727 randomly sampled palm-farm pixels for summer 2024. Palm farms in the Near Urban zone (n = 722) exhibited a mean NDVI of 0.442 ± 0.171, indicating sparse-to-moderate vegetation density, and a mean NDMI of 0.124 ± 0.092, which falls within the Moderate Moisture class (0.12–0.25), only marginally above the Mild Water Stress upper limit (0.12). Pixel-level NDMI ranged from −0.116 to 0.360, spanning the Severe Water Stress to High Moisture classes, indicating considerable within-zone heterogeneity. The Medium Urban zone (n = 5) recorded slightly higher mean NDVI (0.525 ± 0.220) but lower mean NDMI (0.088 ± 0.067), which falls within the Mild Water Stress class, suggesting greater moisture stress despite maintained vegetation greenness. All results for the Medium Urban zone are treated as exploratory due to the small sample size.

Table 2. Descriptive Statistics of LST, NDVI, and NDMI by Buffer Zone — Palm-Farm Sample (Summer 2024, n = 727)

Index	Zone	n	Mean	SD	Min	Max
LST (°C)	Near Urban	722	47.21	3.06	40.67	57.28
LST (°C)	Medium Urban†	5	50.87	1.80	49.22	52.97
NDVI	Near Urban	722	0.442	0.171	0.044	0.833
NDVI	Medium Urban†	5	0.525	0.220	0.255	0.770
NDMI	Near Urban	722	0.124	0.092	-0.116	0.360
NDMI	Medium Urban†	5	0.088	0.067	-0.007	0.136

†Medium Urban zone: n = 5; results are exploratory only. Source: Sentinel-2 SR Harmonized & Landsat 9 Level-2, processed via Google Earth Engine.

4.4. Spatiotemporal Vegetation Change (2017–2024)

Between 2017 and 2024, mean NDVI across all palm-farm pixels showed a near-zero change (Δ = +0.009), indicating aggregate stability at the oasis scale. However, the NDVI change map (Figure 5b) reveals substantial spatial heterogeneity: moderate NDVI decreases (−0.30 to 0.00) prevailed across the majority of palm-farm areas, particularly near high-density urban zones, while localized increases (0.00 to +0.40) were observed in scattered agricultural parcels, suggesting variable land management responses across the oasis.

This spatial heterogeneity is masked by the near-zero aggregate mean. The LST change map (Figure 5a) shows a similarly heterogeneous pattern: moderate warming (0–5°C) dominated central and southern agricultural zones, strong warming (5–10.9°C) was evident along the eastern urban fringe, and localized cooling (−14 to −5°C) was concentrated in the northern sector, likely associated with changes in irrigation intensity or land management practices.

Volume 8 – Issue 85
Issued on: 20 November 2026
International Journal of Research and Studies Publishing
المجلة الدولية لنشر البحوث والدراسات
ISSN: 2709-7064

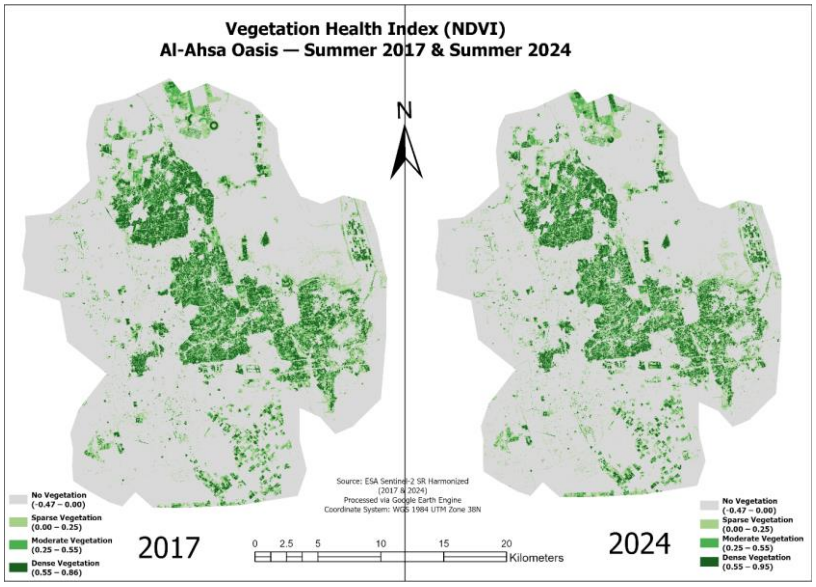

Figure 3. Spatial distribution of NDVI in Al-Ahsa Oasis during summer 2017 (a) and summer 2024 (b). NDVI values range from −0.47 (bare surfaces) to 0.86–0.95 (dense palm vegetation). Dense vegetation clusters are concentrated in the central agricultural zones of Hofuf and Mubarraz, while sparse vegetation is distributed along the urban fringe. Mean NDVI change (Δ = +0.009) across palm-farm pixels indicates near-zero aggregate change, masking substantial spatial heterogeneity.

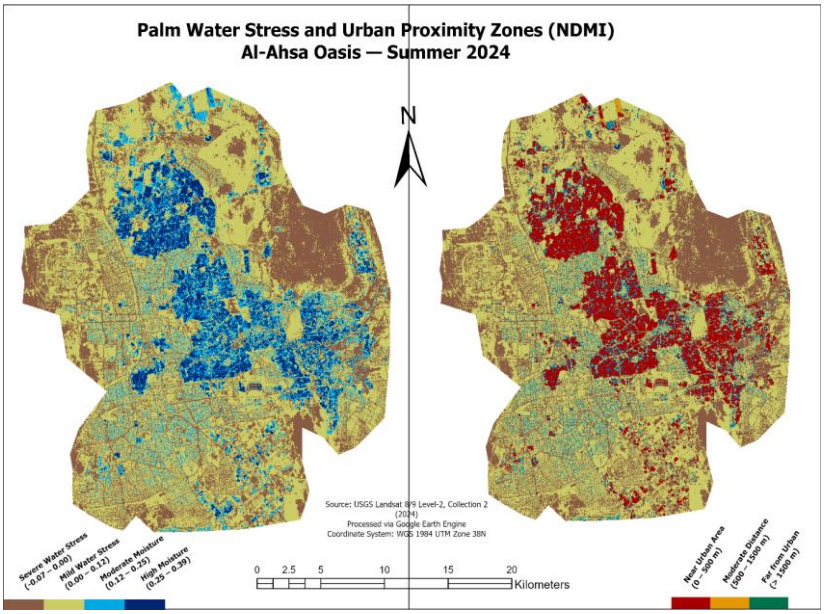

Figure 4. Spatial distribution of palm water stress (NDMI) and urban proximity buffer zones in Al-Ahsa Oasis during summer 2024. NDMI classification: Severe Water Stress (< −0.07; observed minimum −0.116); Mild Water Stress (−0.07 to 0.12); Moderate Moisture (0.12–0.25); High Moisture (> 0.25). Severe water stress zones are scattered along the urban–agricultural interface. Buffer zone map confirms 99.3% of sampled pixels within the Near Urban zone.

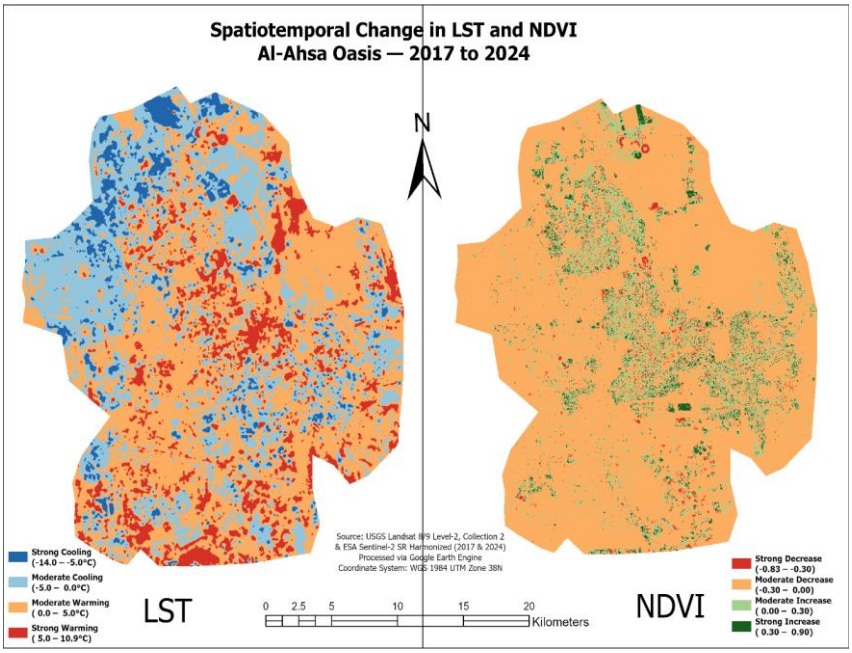

Figure 5. Spatiotemporal change in LST (a) and NDVI (b) in Al-Ahsa Oasis between 2017 and 2024.

4.5 Coupled Thermal–Vegetation–Moisture Responses

Pearson correlation analysis across 727 palm-farm pixels revealed significant relationships among all three indices (Table 3). LST was significantly and negatively correlated with NDVI ($r = -0.316$, $R^2 = 0.100$, $p < 0.001$), though surface temperature explains only 10.0% of the variance in vegetation greenness. A substantially stronger negative correlation was observed between LST and NDMI ($r = -0.599$, $R^2 = 0.359$, $p < 0.001$), with surface temperature accounting for 35.9% of the variance in canopy moisture condition. The strongest relationship was found between NDVI and NDMI ($r = +0.829$, $R^2 = 0.687$, $p < 0.001$), confirming tight coupling between greenness and moisture retention. The key finding is that NDMI responds more directly to thermal exposure than NDVI, suggesting that moisture decline may precede visible canopy degradation—a critical distinction for oasis conservation monitoring.

Table 3. Pearson Correlation Coefficients between LST, NDVI, and NDMI (n = 727 palm-farm pixels, summer 2024)

Variable Pair	r	R^2	p-value	Significance
LST vs. NDVI	−0.316	0.100	2.63×10^{-18}	***
LST vs. NDMI	−0.599	0.359	5.11×10^{-72}	***
NDVI vs. NDMI	+0.829	0.687	6.76×10^{-185}	***

*** $p < 0.001$. R^2 = coefficient of determination. Source: Author's calculations.

4.6. Spatial Detection of Palm Stress Hotspots

The integration of LST, NDVI, and NDMI provides a spatially explicit basis for identifying hidden palm stress hotspots across Al-Ahsa Oasis. The most vulnerable areas were defined not by a single index, but by the spatial overlap of elevated surface temperature, reduced moisture condition, and declining vegetation greenness. These overlapping stress signals were concentrated mainly along fragmented urban-fringe parcels and peripheral agricultural zones. Dense and continuous palm clusters appear to retain localized cooling capacity through transpirational cooling and canopy shading, whereas fragmented and urban-fringe parcels are more exposed to heat accumulation and moisture decline. The oasis should therefore be understood as a mosaic of resilient and vulnerable palm-farm patches, where localized stress may be obscured by spatially averaged NDVI values.

5. Discussion

5.1. Urban Oasis Vulnerability under Hyper-Arid Thermal Conditions

The documented increase of +1.81°C in mean LST over palm-farm pixels in the Near Urban zone (0–500 m) between 2017 and 2024 is consistent with documented warming trajectories across Saudi Arabia's Eastern Province (Hassaballa & Salih, 2023; Assiri et al., 2025) and with global projections of accelerated warming in arid urban environments (Lazzarini et al., 2013). In hyper-arid settings, the thermal contrast between vegetated and built-up surfaces is amplified by the absence of evapotranspiration over bare and impervious areas. The spatial heterogeneity observed in the LST change map—with moderate warming dominating central agricultural zones and strong warming (5–10.9°C) concentrated along the eastern urban fringe—reflects the progressive fragmentation of the oasis agricultural fabric by expanding impervious surfaces. This pattern aligns with the documented 170% increase in built-up area cover in Al-Ahsa between 1990 and 2020 (Hassaballa & Salih, 2023) and confirms that the oasis is transitioning from a contiguous cooling landscape to a thermally fragmented mosaic. The localized cooling (−14 to −5°C) observed in the northern sector likely reflects changes in irrigation management or local land cover transitions, rather than a regional cooling trend, and warrants further investigation.

5.2. NDMI as an Early-Warning Indicator of Date Palm Stress

The substantially stronger correlation between LST and NDMI ($r = -0.599$, $R^2 = 0.359$) compared to LST and NDVI ($r = -0.316$, $R^2 = 0.100$) provides empirical support for the use of canopy moisture indices as early-warning tools in irrigated date palm systems. This differential sensitivity arises from the physiological architecture of date palm stress response: stomatal conductance and transpirational

cooling are disrupted by elevated temperatures before visible canopy degradation occurs (Kruse et al., 2019; Paoletti et al., 2021). In irrigated oasis systems, drip or falaj irrigation can temporarily sustain canopy greenness while internal moisture deficits compound, a mechanism that NDVI cannot detect. The observation that the Medium Urban zone recorded lower mean NDMI (0.088, Mild Water Stress class) despite higher mean NDVI (0.525), compared with the Near Urban zone (NDMI = 0.124, Moderate Moisture class, marginally above the 0.12 threshold; NDVI = 0.442), illustrates this decoupling in practice. This observation should be interpreted cautiously due to the limited sample size of the Medium Urban zone. These results are consistent with the documented association between high summer temperatures (>48°C) and Date Fruit Unripening Syndrome in the 'Khalas' cultivar (Iqbal et al., 2025), which manifests as a cumulative production-level outcome of moisture stress rather than immediate canopy collapse. Relying on NDVI alone in conservation assessments could therefore produce an overly optimistic interpretation of oasis stability.

5.3. Limits of Vegetation Cooling in Irrigated Arid Landscapes

The strong positive correlation between NDVI and NDMI ($r = +0.829$, $R^2 = 0.687$) confirms the tight coupling between vegetation greenness and moisture retention. However, the spatial analysis reveals that this coupling is not uniformly protective. Dense and continuous palm clusters in the central agricultural zones of Hofuf and Mubarraz demonstrated lower LST values, consistent with the oasis cool island effect through canopy shading and evapotranspiration (Boudjellal et al., 2025; Boudjellal & Bourbia, 2018). In contrast, fragmented and peripheral parcels along the urban–agricultural interface showed NDMI values approaching severe water stress thresholds, indicating that spatial fragmentation limits the collective cooling capacity of the oasis. Where farm parcels are small, isolated, or immediately adjacent to impervious surfaces, the transpirational cooling capacity of individual palms is overwhelmed by radiative heat loading from surrounding built-up surfaces. The mean NDVI change near zero ($\Delta = +0.009$) masks this spatial heterogeneity: aggregate greenness stability coexists with localized and progressive moisture stress in the most vulnerable parcels.

5.4. Thermal Stress–Vegetation Relationships

The analysis further supports the observed relationships between thermal conditions and vegetation responses across Al-Ahsa Oasis. While increasing LST was associated with reductions in both NDVI and NDMI, the stronger explanatory power observed for NDMI indicates that canopy moisture conditions are more sensitive to thermal stress than vegetation greenness. This finding is consistent with previous studies showing that physiological moisture decline often precedes visible canopy

degradation in irrigated agricultural systems. Consequently, NDMI provides a more reliable indicator for the early detection of heat-related stress in date palm agroecosystems.

5.5. Planning Implications for Al-Ahsa Oasis Conservation

The spatially explicit identification of thermal stress hotspots at the urban–agricultural interface provides a quantitative basis for prioritizing conservation interventions. Palm farm parcels along the eastern urban fringe, where strong warming (5–10.9°C increase) and NDVI decline were simultaneously observed, should be designated as priority zones for remedial action. Evidence-based recommendations include: (1) establishing vegetated green buffer zones along newly developed urban boundaries to attenuate radiative heat loading on adjacent palm parcels; (2) integrating NDMI monitoring into existing agricultural management frameworks to enable early detection of moisture stress before visible canopy degradation occurs; and (3) preserving contiguous palm canopy blocks—which retain localized cooling capacity—as a binding criterion in urban planning approvals. These recommendations are directly aligned with the sustainable agriculture and heritage conservation objectives of Saudi Vision 2030 and with the Outstanding Universal Value commitments of the UNESCO World Heritage designation of Al-Ahsa Oasis (UNESCO, 2018). The documented loss of approximately 27.30 km² of Al-Ahsa vegetation cover between 2014 and 2023 (Assiri et al., 2025) underscores the urgency of integrating remote sensing-based stress monitoring into the oasis management framework.

5.6. Limitations and Future Improvements

Several limitations should be acknowledged. First, the buffer zone analysis was constrained by the spatial distribution of palm pixels: the highly intermingled urban–agricultural configuration of Al-Ahsa Oasis resulted in 99.3% of sampled pixels falling in the Near Urban zone, with only 0.8% (878 pixels) and 3 palm pixels in the Medium and Far Urban zones, respectively, of the full palm-pixel population (5 sampled pixels in the medium zone). All statistical comparisons involving the Medium Urban zone are therefore exploratory and should not be generalized without further sampling. Second, the analysis is based on summer-season imagery only, capturing peak thermal stress but not seasonal variability in palm stress responses. Third, no field-based validation of LST retrieval accuracy or palm physiological stress indicators was conducted; absolute temperature and index values should be interpreted with this caveat. Fourth, the use of two sensor systems (Landsat 8/9 for LST and Sentinel-2 for NDVI/NDMI) introduces potential temporal and spatial resolution inconsistencies. Fifth, palm-farm vegetation was delineated from the ESA WorldCover tree-cover class (10 m), which does not

discriminate date palms from other tree cover and was not validated against field data; the mask was held constant across 2017 and 2024, so changes in palm extent are not captured, and the 10 m mask was applied on the 30 m thermal grid, so some pixels may mix surfaces. Sixth, 2017 LST was derived from Landsat 8 and 2024 LST from Landsat 9, and inter-sensor differences were not harmonized. Future research should employ adaptive zoning strategies with denser sampling across all buffer distances, incorporate multi-seasonal imagery to assess annual stress cycles, and integrate ground-based physiological measurements (Fv/Fm, stomatal conductance) for index validation.

6. Conclusion

This study provides spatiotemporal evidence that urban heat island dynamics are exerting measurable thermal and moisture stress on date palm agroecosystems in Al-Ahsa Oasis between 2017 and 2024. Three principal findings emerge from the analysis. First, mean LST in palm-farm pixels within the Near Urban zone (0–500 m from built-up areas) increased by +1.81°C over the study period, with spatially heterogeneous warming concentrated along the eastern urban fringe and strong cooling anomalies observed in the northern sector. Second, NDMI demonstrated a significantly stronger response to thermal exposure ($r = -0.599$, $R^2 = 0.359$) than NDVI ($r = -0.316$, $R^2 = 0.100$), indicating that canopy moisture conditions are more sensitive to thermal exposure than vegetation greenness, which establishes NDMI as an effective early-warning indicator of heat-induced moisture stress in irrigated date palm systems. Third, the near-zero aggregate NDVI change ($\Delta = +0.009$) masks substantial spatial heterogeneity, with progressive moisture stress and vegetation decline concentrated at fragmented urban-fringe parcels. Collectively, these findings support the development of spatially targeted conservation interventions—including NDMI-based stress monitoring protocols, green buffer zone establishment, and canopy continuity preservation policies—within the framework of Saudi Vision 2030 and UNESCO World Heritage commitments. Future research should extend this analysis to multi-seasonal datasets and integrate field-based physiological validation to strengthen the quantitative basis for oasis conservation management.

7. Declarations

Ethics approval and consent to participate: Not applicable.

Consent for publication: All authors have reviewed the final manuscript and consent to its submission and publication. The article contains no unlawful, defamatory, or otherwise prohibited material that would violate the terms and conditions of publication.

Availability of data and materials: The datasets generated and analyzed during the current study are available from the corresponding author upon reasonable request.

Competing interests: The authors declare that they have no competing interests.

Funding: This research did not receive any specific grant from funding agencies in the public, commercial, or not-for-profit sectors.

8. References

Almadini, A. M., & Hassaballa, A. A. (2019). Depicting changes in land surface cover at Al-Hassa oasis of Saudi Arabia using remote sensing and GIS techniques. *PLoS ONE, 14*(11), e0221115.

Assiri, M. A., et al. (2025). Spatio-temporal dynamics of vegetation and land surface temperature in Saudi Arabia: Impacts of climate change on agricultural sites from 2010 to 2023. *International Journal of Climatology*. https://doi.org/10.1002/joc.8781

Avdan, U., & Jovanovska, G. (2016). Algorithm for automated mapping of land surface temperature using LANDSAT 8 satellite data. *Journal of Sensors, 2016*(1), 1480307.

Boudjellal, L., Boudraa, H., Djaghrouri, D., & Bouafia, A. (2025). Oasis landscape: A valuable urban sustainability solution in arid lands. *Glasnik Srpskog geografskog drustva, 105*(1), 59–66.

Boudjellal, L., & Bourbia, F. (2018). An evaluation of the cooling effect efficiency of the oasis structure in a Saharan town through remotely sensed data. *International Journal of Environmental Studies, 75*(2), 309–320.

de Souza, V. F., et al. (2025). High temperature acclimation of isoprene emission in date palm is associated with enhanced substrate availability and reduction in synthase activity. *Physiologia Plantarum, 177*(3), e70256.

European Space Agency. (2021). *ESA WorldCover v2.0*. https://worldcover2021.esa.int

Gao, B.-C. (1996). NDWI—A normalized difference water index for remote sensing of vegetation liquid water from space. *Remote Sensing of Environment, 58*(3), 257–266.

Gorelick, N., et al. (2017). Google Earth Engine: Planetary-scale geospatial analysis for everyone. *Remote Sensing of Environment, 202*, 18–27.

Hassaballa, A., & Salih, A. (2023). A spatio-temporal analysis of heat island intensity influenced by the substantial urban growth between 1990 and 2020: A case study of Al-Ahsa Oasis, Eastern Saudi Arabia. *Applied Sciences, 13*(5), 2755.

Iqbal, Z., et al. (2025). Environmental drivers of date fruit unripening syndrome in dryland regions of Saudi Arabia. *Frontiers in Plant Science, 16*, 1587061.

Karnieli, A., et al. (2010). Use of NDVI and land surface temperature for drought assessment: Merits and limitations. *Journal of Climate, 23*(3), 618–633.

Kruse, J., et al. (2019). Optimization of photosynthesis and stomatal conductance in the date palm *Phoenix dactylifera* during acclimation to heat and drought. *New Phytologist, 223*(4), 1973–1988.

Lazzarini, M., Marpu, P. R., & Ghedira, H. (2013). Temperature-land cover interactions: The inversion of urban heat island phenomenon in desert city areas. *Remote Sensing of Environment, 130*, 136–152.

Paoletti, E., et al. (2021). Date palm responses to a chronic, realistic ozone exposure in a FACE experiment. *Environmental Research, 195*, 110868.

Salih, A., Hassaballa, A., & Rahma, A. E. (2025). Satellite-derived multi-temporal palm trees and urban cover changes to understand drivers of changes in agroecosystem in Al-Ahsa Oasis using a spectral mixture analysis (SMA) model. *Agriculture, 15*(19), 2043.

Sekertekin, A., & Bonafoni, S. (2020). Land surface temperature retrieval from Landsat 5, 7, and 8 over rural areas. *Remote Sensing, 12*(2), 294.

Sishodia, R. P., Ray, R. L., & Singh, S. K. (2020). Applications of remote sensing in precision agriculture: A review. *Remote Sensing, 12*(19), 3136.

UNESCO. (2018). *Al-Ahsa Oasis, an evolving cultural landscape*. UNESCO World Heritage List. https://whc.unesco.org/en/list/1563

United Nations. (2018). *World urbanization prospects: The 2018 revision*. Department of Economic and Social Affairs, Population Division.

United States Geological Survey. (2024). *Landsat Collection 2 Level-2 science product*. https://www.usgs.gov/landsat-missions

Yaish, M. W., & Halo, B. A. (2026). Date palm (*Phoenix dactylifera* L.) responses to heat stress. In *Soil microorganisms for plant growth promotion and soil health* (pp. 557–584). Elsevier.

Copyright © 2026 (Nawaf Nader, Alyaa Zidan, Rawan Al Nughaymish, Basim Al Sahabi). This article is licensed under the Creative Commons Attribution-NonCommercial 4.0 International License (CC BY-NC 4.0).

Doi: https://doi.org/10.52133/ijrsp.v8.85.4